19

Singularity Robust Inverse Dynamics of Parallel Manipulators

S. Kemal Ider
Middle East Technical University Ankara, Turkey

1. Introduction

Parallel manipulators have received wide attention in recent years. Their parallel structures offer better load carrying capacity and more precise positioning capability of the end-effector compared to open chain manipulators. In addition, since the actuators can be placed closer to the base or on the base itself the structure can be built lightweight leading to faster systems (Gunawardana & Ghorbel, 1997; Merlet, 1999; Gao et al., 2002).

It is known that at *kinematic singular positions* of serial manipulators and parallel manipulators, arbitrarily assigned end-effector motion cannot in general be reached by the manipulator and consequently at those configurations the manipulator loses one or more degrees of freedom. In addition, the closed loop structure of parallel manipulators gives rise to another type of degeneracy, which can be called *drive singularity,* where the actuators cannot influence the end-effector accelerations instantaneously in certain directions and the actuators lose the control of one or more degrees of freedom. The necessary actuator forces become unboundedly large unless consistency of the dynamic equations are guaranteed by the specified trajectory.

The previous studies related to the drive singularities mostly aim at finding only the locations of the singular positions for the purpose of avoiding them in the motion planning stage (Sefrioui & Gosselin, 1995; Daniali et al, 1995; Alici, 2000; Ji, 2003; DiGregorio, 2001; St-Onge & Gosselin, 2000). However unlike the kinematic singularities that occur at workspace boundaries, drive singularities occur inside the workspace and avoiding them limits the motion in the workspace. Therefore, methods by which the manipulator can move through the drive singular positions in a stable fashion are necessary.

This chapter deals with developing a methodology for the inverse dynamics of parallel manipulators in the presence of drive singularities. To this end, the conditions that should be satisfied for the consistency of the dynamic equations at the singular positions are derived. For the trajectory of the end-effector to be realizable by the actuators it should be designed to satisfy the *consistency conditions*. Furthermore, for finding the appropriate actuator forces when drive singularities take place, the dynamic equations are modified by using higher order derivative information. The linearly dependent equations are replaced by the *modified equations* in the neighborhoods of the singularities. Since the locations of the drive singularities and the corresponding modified equations are known (as derived in Section 3), in a practical scenario the actuator forces are found using the modified equations

Source: Parallel Manipulators, New Developments, Book edited by: Jee-Hwan Ryu, ISBN 978-3-902613-20-2, pp. 498, April 2008, I-Tech Education and Publishing, Vienna, Austria

in the vicinity of the singular positions and using the regular inverse dynamic equations elsewhere. Deployment motions of 2 and 3 dof planar manipulators are analyzed to illustrate the proposed approach (Ider, 2004; Ider, 2005).

2. Inverse dynamics and singular positions

Consider an n degree of freedom parallel robot. Let the system be converted into an open-tree structure by disconnecting a sufficient number of unactuated joints. Let the degree of freedom of the open-tree system be *m*, i.e. the number of the independent loop closure constraints in the parallel manipulator be m-n. Let $\boldsymbol{\eta} = [\eta_1,...,\eta_m]^T$ denote the joint variables of the open-tree system and $\mathbf{q} = [q_1,...,q_n]^T$ the joint variables of the actuated joints. The *m-n* loop closure equations, obtained by reconnecting the disconnected joints, can be written as

$$\phi_i(\eta_1,...,\eta_m) = 0 \qquad i=1,...,m\text{-}n \tag{1}$$

and can be expressed at velocity level as

$$\Gamma^G_{ij}\,\dot{\eta}_j = 0 \qquad i=1,...,m\text{-}n \qquad j=1,...,m \tag{2}$$

where $\Gamma^G_{ij} = \dfrac{\partial \phi_i}{\partial \eta_j}$. A repeated subscript index in a term implies summation over its range. The prescribed end-effector Cartesian variables $x_i(t)$, $i=1,...,n$ represent the tasks of the non-redundant manipulator. The relations between the joint variables due to the tasks are

$$f_i(\eta_1,...,\eta_m) = x_i \qquad i=1,...,n \tag{3}$$

Equation (3) can be written at velocity level as

$$\Gamma^P_{ij}\,\dot{\eta}_j = \dot{x}_i \qquad i=1,...,n \qquad j=1,...,m \tag{4}$$

where $\Gamma^P_{ij} = \dfrac{\partial f_i}{\partial \eta_j}$. Equations (2) and (4) can be written in combined form,

$$\boldsymbol{\Gamma}\,\dot{\boldsymbol{\eta}} = \mathbf{h} \tag{5}$$

where $\boldsymbol{\Gamma}^{\mathrm{T}} = \left[\boldsymbol{\Gamma}^{G^{\mathrm{T}}} \quad \boldsymbol{\Gamma}^{P^{\mathrm{T}}}\right]$ which is an $m \times m$ matrix and $\mathbf{h}^{\mathrm{T}} = \left[\mathbf{0} \quad \dot{\mathbf{x}}^{\mathrm{T}}\right]$. The derivative of equation (5) gives the acceleration level relations,

$$\boldsymbol{\Gamma}\,\ddot{\boldsymbol{\eta}} = -\dot{\boldsymbol{\Gamma}}\,\dot{\boldsymbol{\eta}} + \dot{\mathbf{h}} \tag{6}$$

The dynamic equations of the parallel manipulator can be written as

$$\mathbf{M}\,\ddot{\boldsymbol{\eta}} - \boldsymbol{\Gamma}^{G^{\mathrm{T}}}\boldsymbol{\lambda} - \mathbf{Z}^{\mathrm{T}}\,\mathbf{T} = \mathbf{R} \tag{7}$$

where **M** is the $m \times m$ generalized mass matrix and **R** is the vector of the generalized Coriolis, centrifugal and gravity forces of the open-tree system, $\boldsymbol{\lambda}$ is the $(m-n)\times 1$ vector of the joint forces at the loop closure joints, **T** is the $n \times 1$ vector of the actuator forces, and each row of **Z** is the direction of one actuator force in the generalized space. If the variable of the joint which is actuated by the *i* th actuator is η_k, then for the *i* th row of **Z**, $Z_{ik} = 1$ and $Z_{ij} = 0$ for j=1,...,m ($j \neq k$).

Combining the terms involving the unknown forces $\boldsymbol{\lambda}$ and **T**, one can write equation (7) as

$$\mathbf{A}^{\mathrm{T}} \boldsymbol{\tau} = \mathbf{M}\ddot{\boldsymbol{\eta}} - \mathbf{R} \tag{8}$$

where the $\mathrm{m} \times \mathrm{m}$ matrix $\mathbf{A}^{\mathrm{T}}$ and the $m \times 1$ vector $\boldsymbol{\tau}$ are

$$\mathbf{A}^{\mathrm{T}} = \begin{bmatrix} \boldsymbol{\Gamma}^{G^{\mathrm{T}}} & \mathbf{Z}^{\mathrm{T}} \end{bmatrix} \tag{9}$$

and

$$\boldsymbol{\tau}^{\mathrm{T}} = \begin{bmatrix} \boldsymbol{\lambda}^{\mathrm{T}} & \mathbf{T}^{\mathrm{T}} \end{bmatrix} \tag{10}$$

The inverse dynamic solution of the system involves first finding $\ddot{\boldsymbol{\eta}}$, $\dot{\boldsymbol{\eta}}$ and $\boldsymbol{\eta}$ from the kinematic equations and then finding $\boldsymbol{\tau}$ (and hence **T**) from equation (8).

For the prescribed **x**(t), $\ddot{\boldsymbol{\eta}}$ can be found from equation (6), $\dot{\boldsymbol{\eta}}$ from equation (5) and $\boldsymbol{\eta}$ can be found either from the position equations (1,3) or by numerical integration. However during the inverse kinematic solution, singularities occur when $|\boldsymbol{\Gamma}| = 0$. At these configurations, the assigned $\dot{\mathbf{x}}$ cannot in general be reached by the manipulator since, in equation (3), a vector **h** lying outside the space spanned by the columns of $\boldsymbol{\Gamma}$ cannot be produced and consequently the manipulator loses one or more degrees of freedom.

Singularities may also occur while solving for the actuator forces in the dynamic equation (8), when $|\mathbf{A}| = 0$. For each different set of actuators, **Z** hence the singular positions are different. Because this type of singularity is associated with the locations of the actuators, it is called *drive singularity* (or *actuation singularity*). At a drive singularity the assigned $\ddot{\boldsymbol{\eta}}$ cannot in general be realized by the actuators since, in equation (8), a right hand side vector lying outside the space spanned by the columns of $\mathbf{A}^{\mathrm{T}}$ cannot be produced, i.e. the actuators cannot influence the end-effector accelerations instantaneously in certain directions and the actuators lose the control of one or more degrees of freedom. (The system cannot resist forces or moments in certain directions even if all actuators are locked.) The actuator forces become unboundedly large unless consistency of the dynamic equations are guaranteed by the specified trajectory.

Let $\boldsymbol{\Gamma}^{Gu}$ be the $(m-n)\times(m-n)$ matrix which is composed of the columns of $\boldsymbol{\Gamma}^{G}$ that correspond to the variables of the unactuated joints. Since $Z_{ik} = 1$ and $Z_{ij} = 0$ for $j \neq k$, the drive singularity condition $|\mathbf{A}| = 0$ can be equivalently written as $|\boldsymbol{\Gamma}^{\mathrm{Gu}}| = 0$.

In the literature the singular positions of parallel manipulators are mostly determined using the kinematic expression between $\dot{\mathbf{q}}$ and $\dot{\mathbf{x}}$ which is obtained by eliminating the variables

of the unactuated joints (Sefrioui & Gosselin, 1995; Daniali et al, 1995; Alici, 2000; Ji, 2003; DiGregorio, 2001; St-Onge & Gosselin, 2000),

$$\mathbf{J}\dot{\mathbf{q}} + \mathbf{K}\dot{\mathbf{x}} = \mathbf{0} \tag{11}$$

References (Sefrioui & Gosselin, 1995 ; Daniali et al, 1995; Ji, 2003) name the condition $|\mathbf{J}| = 0$ as "Type I singularity" and the condition $|\mathbf{K}| = 0$ "Type II singularity". And in reference (DiGregorio, 2001) they are called "inverse problem singularity" and "direct problem singularity", respectively. Since it shows the lost Cartesian degrees of freedom, the condition $|\mathbf{\Gamma}| = 0$ shown above corresponds to $|\mathbf{J}| = 0$. For the drive singularity, equation (2) can be written as

$$\mathbf{\Gamma}^{Gu}\dot{\boldsymbol{\eta}}^{u} = -\mathbf{\Gamma}^{Ga}\dot{\mathbf{q}} \tag{12}$$

where $\boldsymbol{\eta}^{u}$ is the vector of the joint variables of the unactuated joints and $\mathbf{\Gamma}^{Ga}$ is the matrix composed of the columns of $\mathbf{\Gamma}^{G}$ associated with the actuated joints. Since after finding $\dot{\boldsymbol{\eta}}^{u}$ from eqn (12) one can find $\mathbf{h}$ and hence $\dot{\mathbf{x}}$ from eqn (5) directly, the drive singularity condition $|\mathbf{A}| = 0$ (i.e. $|\mathbf{\Gamma}^{\mathrm{Gu}}| = 0$) given above is equivalent to $|\mathbf{K}| = 0$. It should be noted that the identification of the singular configurations as shown here is easier since elimination of the variables of the passive joints is not necessary.

3. Consistency conditions and modified equations

At the motion planning stage one usually tries to avoid singular positions. This is not difficult as far as inverse kinematic singularities are concerned because they usually occur at the workspace boundaries (DiGregorio, 2001). In this paper it is assumed that $\mathbf{\Gamma}$ always has full rank, i.e. the desired motion is chosen such that the system never comes to an inverse kinematic singular position. On the other hand, drive singularities usually occur inside the workspace and avoiding them restricts the functional workspace. It is therefore important to devise techniques for passing through the singular positions while the stability of the control forces is maintained. To this end, equation (8) must be made consistent at the singular position. In other words, since the rows of $\mathbf{A}^{\mathrm{T}}$ become linearly dependent, the same relation must also be present between the rows of the right hand side vector ($\mathbf{M}\ddot{\boldsymbol{\eta}} - \mathbf{R}$), so that it lies in the vector space spanned by the columns of $\mathbf{A}^{\mathrm{T}}$.

3.1 Consistency conditions and modified equations when rank(A) becomes m-1

At a drive singularity, usually rank of $\mathbf{A}$ becomes m-1. Let at the singular position the s th row of $\mathbf{A}^{\mathrm{T}}$ become a linear combination of the other rows of $\mathbf{A}^{\mathrm{T}}$.

$$A^{\mathrm{T}}_{sj} = \alpha_p A^{\mathrm{T}}_{pj} \qquad p = 1,...,m \quad (p \neq s)\,, \quad j = 1,...,m \tag{13}$$

where α_p are the linear combination coefficients (which may depend also on η_i). Notice that only those rows of $\mathbf{A}^{\mathrm{T}}$ which are associated with the unactuated joints can become

linearly dependent, hence α_p corresponding to the actuated joints are zero. Then for the rows of equation (6) one must have

$$A_{sj}^{\mathrm{T}}\,\tau_j - \alpha_p\,A_{pj}^{\mathrm{T}}\,\tau_j = M_{sj}\,\ddot{\eta}_j - R_s - \alpha_p(M_{pj}\,\ddot{\eta}_j - R_p) \tag{14}$$

Substitution of equation (13) into equation (14) yields

$$M_{sj}\,\ddot{\eta}_j - R_s = \alpha_p(M_{pj}\,\ddot{\eta}_j - R_p) \tag{15}$$

Equation (15) represents the *consistency condition* that $\ddot{\eta}_j$ should satisfy at the singular position. Since $\ddot{\eta}_j$ are obtained from the inverse kinematic equations (6), the trajectory $\ddot{\mathbf{x}}$ must be planned in such a way to satisfy equation (15) at the drive singularity. Otherwise an inconsistent trajectory cannot be realized and the actuator forces grow without bounds as the drive singularity is approached. Time derivative of equation (14) is

$$(A_{sj}^{\mathrm{T}} - \alpha_p\,A_{pj}^{\mathrm{T}})\,\dot{\tau}_j + (\dot{A}_{sj}^{\mathrm{T}} - \alpha_p\,\dot{A}_{pj}^{\mathrm{T}} - \dot{\alpha}_p\,A_{pj}^{\mathrm{T}})\,\tau_j = (M_{sj} - \alpha_p M_{pj})\,\dddot{\eta}_j$$

$$+(\dot{M}_{sj} - \alpha_p\dot{M}_{pj} - \dot{\alpha}_p M_{pj})\,\ddot{\eta}_j - \dot{R}_s + \alpha_p\dot{R}_p + \dot{\alpha}_p R_p \tag{16}$$

Now, because equation (13) holds at the singular position, there exists a neighborhood in which the first term in equation (16) is negligible compared to the other terms. Therefore in that neighborhood this term can be dropped to yield

$$(\dot{A}_{sj}^{\mathrm{T}} - \alpha_p\,\dot{A}_{pj}^{\mathrm{T}} - \dot{\alpha}_p\,A_{pj}^{\mathrm{T}})\,\tau_j = (M_{sj} - \alpha_p M_{pj})\,\dddot{\eta}_j + (\dot{M}_{sj} - \alpha_p\dot{M}_{pj} - \dot{\alpha}_p M_{pj})\,\ddot{\eta}_j - \dot{R}_s + \alpha_p\dot{R}_p + \dot{\alpha}_p R_p \tag{17}$$

Equation (17) is the *modified equation* that can be used to replace the s th row of equation (8) or any other equation in the linearly dependent set.

3.2 Consistency conditions and modified equations when rank(A) becomes r<m

In the general case where the rank of $\mathbf{A}^{\mathrm{T}}$ becomes $r < m$ at the singular position, let rows s_k, $k = 1,...,m\text{-}r$ of $\mathbf{A}^{\mathrm{T}}$ become linear combinations of the other r rows of $\mathbf{A}^{\mathrm{T}}$,

$$A_{s_k j}^{\mathrm{T}} = \alpha_{kp}\,A_{pj}^{\mathrm{T}} \qquad p = 1,...,m \quad (p \neq s_k), \quad j = 1,...,m, \quad k = 1,...,m\text{-}r \tag{18}$$

where α_{kp} are the linear combination coefficients. Then the following relations must be present among the rows of equation (8)

$$A_{s_k j}^{\mathrm{T}}\,\tau_j - \alpha_{kp}\,A_{pj}^{\mathrm{T}}\,\tau_j = M_{s_k j}\,\ddot{\eta}_j - R_{s_k} - \alpha_{kp}(M_{pj}\,\ddot{\eta}_j - R_p) \qquad k = 1,...,m\text{-}r \tag{19}$$

The consistency relations are obtained as below

$$M_{s_k j}\,\ddot{\eta}_j - R_{s_k} = \alpha_{kp}(M_{pj}\,\ddot{\eta}_j - R_p) \qquad k = 1,...,m\text{-}r \tag{20}$$

Substitution of equation (18) into the derivative of equation (19) yields the modified equations,

$$(\dot{A}^{\mathrm{T}}_{s_k j} - \alpha_{kp}\,\dot{A}^{\mathrm{T}}_{pj} - \dot{\alpha}_{kp}\,A^{\mathrm{T}}_{pj})\,\tau_j = (M_{s_k j} - \alpha_{kp} M_{pj})\,\ddot{\eta}_j + (\dot{M}_{s_k j} - \alpha_{kp}\dot{M}_{pj} - \dot{\alpha}_{kp} M_{pj})\,\dot{\eta}_j$$

$$-\dot{R}_{s_k} + \alpha_{kp}\dot{R}_p + \dot{\alpha}_{kp} R_p \qquad k = 1,\ldots,m\text{-}r \tag{21}$$

3.3 Inverse dynamics algorithm in the presence of drive singularities

When the linearly dependent dynamic equations in equation (8) are replaced by the modified equations, equation (8) takes the following form, which is valid in the vicinity of the singular configurations.

$$\mathbf{D}^{\mathrm{T}}\,\boldsymbol{\tau} = \mathbf{S} \tag{22}$$

where in the case the s th row of $\mathbf{A}^{\mathrm{T}}$ becomes a linear combination of the other rows,

$$D^{\mathrm{T}}_{ij} = \begin{cases} A^{\mathrm{T}}_{ij} & i \neq s \\ \dot{A}^{\mathrm{T}}_{ij} - \alpha_p \dot{A}^{\mathrm{T}}_{pj} - \dot{\alpha}_p \dot{A}^{\mathrm{T}}_{pj} & i = s \end{cases} \tag{23}$$

and

$$S_i = \begin{cases} M_{ij}\,\dot{\eta}_j - R_i & i \neq s \\ (M_{ij} - \alpha_p M_{pj})\,\ddot{\eta}_j + (\dot{M}_{ij} - \alpha_p \dot{M}_{pj} - \dot{\alpha}_p M_{pj})\,\dot{\eta}_j - \dot{R}_i + \alpha_p \dot{R}_p + \dot{\alpha}_p R_p & i = s \end{cases} \tag{24}$$

In the general case when the rank of $\mathbf{A}^{\mathrm{T}}$ becomes r, $\mathbf{D}^{\mathrm{T}}$ and $\mathbf{S}$ take the following form.

$$D^{\mathrm{T}}_{ij} = \begin{cases} A^{\mathrm{T}}_{ij} & i \neq s_k,\ k = 1,\ldots,m-r \\ \dot{A}^{\mathrm{T}}_{ij} - \alpha_{kp}\dot{A}^{\mathrm{T}}_{pj} - \dot{\alpha}_{kp} A^{\mathrm{T}}_{pj} & i = s_k,\ k = 1,\ldots,m-r \end{cases} \tag{25}$$

and

$$S_i = \begin{cases} M_{ij}\,\dot{\eta}_j - R_i & i \neq s_k,\ k = 1,\ldots,m-r \\ (M_{ij} - \alpha_{kp} M_{pj})\,\ddot{\eta}_j + (\dot{M}_{ij} - \alpha_{kp}\dot{M}_{pj} - \dot{\alpha}_{kp} M_{pj})\,\dot{\eta}_j - \dot{R}_i + \alpha_{kp}\dot{R}_p + \dot{\alpha}_{kp} R_p & i = s_k,\ k = 1,\ldots,m-r \end{cases} \tag{26}$$

Notice that $\ddot{\boldsymbol{\eta}}$ in the modified equation should be found from the derivative of equation (6),

$$\boldsymbol{\Gamma}\,\ddot{\boldsymbol{\eta}} = -2\dot{\boldsymbol{\Gamma}}\,\dot{\boldsymbol{\eta}} - \ddot{\boldsymbol{\Gamma}}\,\dot{\boldsymbol{\eta}} + \ddot{\mathbf{h}} \tag{27}$$

$\ddot{\boldsymbol{\eta}}$ obtained from equation (27) corresponds to the prescribed end-effector jerks $\dddot{\mathbf{x}}$ (in $\ddot{\mathbf{h}}$). Also the coefficients of the forces in the modified equations (17,21) depend on velocities. Therefore, if at the singularity the system is in motion, then by the modified equations the driving forces affect the end-effector jerk instantaneously in the singular directions.

The *inverse dynamics algorithm* in the presence of drive singularities is given below.

1. Find the loci of the positions where the actuation singularities occur and find the linear dependency coefficients associated with the singular positions.
2. If the assigned path of the end-effector passes through singular positions, design the trajectory so as to satisfy the consistency conditions at the singular positions.

3. Set time $t = 0$.
4. Calculate $\boldsymbol{\eta}$, $\dot{\boldsymbol{\eta}}$ and $\ddot{\boldsymbol{\eta}}$ from kinematic equations.
5. If the manipulator is in the vicinity of a singular position, i.e. $|g(\eta_1,...,\eta_m)| < \varepsilon$ where $g(\eta_1,...,\eta_m) = 0$ is the singularity condition and ε is a specified small number, calculate $\ddot{\boldsymbol{\eta}}$ from eqn (27) and then find $\boldsymbol{\tau}$ (hence **T**) from equation (22).
6. If the manipulator is not in the vicinity of a singular position, i.e. $|g(\eta_1,...,\eta_m)| > \varepsilon$, find $\boldsymbol{\tau}$ (hence **T**) from equation (8).
7. Set $t = t + \Delta t$. If the final time is reached, stop. Otherwise continue from step 3.

4. Case studies

4.1 Two degree of freedom 2-RRR planar parallel manipulator

The planar parallel manipulator shown in Figure 1 has 2 degrees of freedom ($n = 2$). Considering disconnection of the revolute joint at *P*, the joint variable vector of the open-chain system is $\boldsymbol{\eta} = [\theta_1 \quad \theta_2 \quad \theta_3 \quad \theta_4]^{\mathrm{T}}$. The joints at *A* and *C* are actuated, i.e. $\mathbf{q} = [\theta_1 \quad \theta_2]^{\mathrm{T}}$. The end point P is desired to make a deployment motion *s*(*t*) along a straight line whose angle with x-axis is $\gamma = 330^o$, starting from initial position $x_{P_o} = -0.431\,\mathrm{m}$, $y_{P_o} = 1.385\,\mathrm{m}$. The time of the motion is $T = 1\,\mathrm{s}$ and its length is $L = 2.3\,\mathrm{m}$ in the positive s sense.

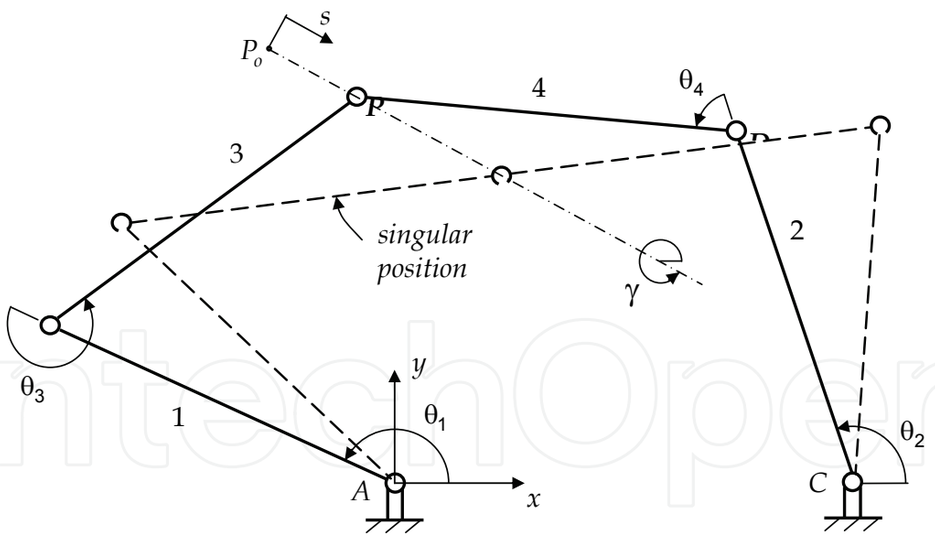

Figure 1. Two degree of freedom 2-RRR planar parallel manipulator.

The moving links are uniform bars. The fixed dimensions are labelled as $r_o = AC$, $r_1 = AB$, $r_2 = CD$, $r_3 = BP$ and $r_4 = DP$. The numerical data are $r_o = 1.75\,\mathrm{m}$, $r_1 = r_2 = r_3 = r_4 = 1.4\,\mathrm{m}$, $m_1 = m_2 = 6\,\mathrm{kg}$ and $m_3 = m_4 = 4\,\mathrm{kg}$.

The loop closure constraint equations at velocity level are $\boldsymbol{\Gamma}^G \dot{\boldsymbol{\eta}} = \mathbf{0}$ where

$$\mathbf{\Gamma}^G = \begin{bmatrix} -r_1 s_1 - r_3 s_{13} & r_2 s_2 + r_4 s_{24} & -r_3 s_{13} & r_4 s_{24} \\ r_1 c_1 + r_3 c_{13} & -r_2 c_2 - r_4 c_{24} & r_3 c_{13} & -r_4 c_{24} \end{bmatrix} \tag{28}$$

Here $s_i = \sin\theta_i$, $c_i = \cos\theta_i$, $s_{ij} = \sin(\theta_i + \theta_j)$, $c_{ij} = \cos(\theta_i + \theta_j)$. The prescribed Cartesian motion of the end point *P*, **x** can be written as

$$\mathbf{x} = \begin{bmatrix} x_P(t) \\ y_P(t) \end{bmatrix} = \begin{bmatrix} x_{P_o} + s(t)\sin\gamma \\ y_{P_o} + s(t)\cos\gamma \end{bmatrix} \tag{29}$$

Then the task equations at velocity level are $\mathbf{\Gamma}^P \dot{\boldsymbol{\eta}} = \dot{\mathbf{x}}$, where

$$\mathbf{\Gamma}^P = \begin{bmatrix} -r_1 s_1 - r_3 s_{13} & 0 & -r_3 s_{13} & 0 \\ r_1 c_1 + r_3 c_{13} & 0 & r_3 c_{13} & 0 \end{bmatrix} \tag{30}$$

The mass matrix **M** and the vector of the Coriolis, centrifugal and gravitational forces **R** are

$$\mathbf{M} = \begin{bmatrix} M_{11} & 0 & M_{13} & 0 \\ 0 & M_{22} & 0 & M_{24} \\ M_{13} & 0 & M_{33} & 0 \\ 0 & M_{24} & 0 & M_{44} \end{bmatrix} \tag{31}$$

where

$$M_{11} = m_1 \frac{r_1^2}{3} + m_3\left(r_1^2 + \frac{r_3^2}{3} + r_1 r_3 c_3\right), \quad M_{13} = m_3\left(\frac{r_3^2}{3} + \frac{r_1 r_3 c_3}{2}\right), \quad M_{33} = m_3 \frac{r_3^2}{3}$$

$$M_{22} = m_2 \frac{r_2^2}{3} + m_4\left(r_2^2 + \frac{r_4^2}{3} + r_2 r_4 c_4\right), \quad M_{24} = m_4\left(\frac{r_4^2}{3} + \frac{r_2 r_4 c_4}{2}\right), \quad M_{44} = m_4 \frac{r_4^2}{3} \tag{32}$$

and

$$\mathbf{R} = \begin{bmatrix} R_1 \\ R_2 \\ R_3 \\ R_4 \end{bmatrix} = \begin{bmatrix} -\,m_3 r_1 r_3 s_3 \dot{\theta}_3 (\dot{\theta}_1 - \frac{1}{2}\dot{\theta}_3) + \frac{1}{2} m_1 g & r_1 c_1 + m_3 g & (r_1 c_1 + \frac{1}{2} r_3 c_{13}) \\ \frac{1}{2} m_3 r_1 r_3 s_3 \dot{\theta}_1^2 + \frac{1}{2} m_3 g & r_3 c_{13} & \\ -\,m_4 r_2 r_4 s_4 \dot{\theta}_4 (\dot{\theta}_2 - \frac{1}{2}\dot{\theta}_4) + \frac{1}{2} m_2 g & r_2 c_2 + m_4 g & (r_2 c_2 + \frac{1}{2} r_4 c_{24}) \\ \frac{1}{2} m_4 r_2 r_4 s_4 \dot{\theta}_2^2 + \frac{1}{2} m_4 g & r_4 c_{24} & \end{bmatrix} \tag{33}$$

Since the variables of the actuated joints are θ_1 and θ_2, the matrix **Z** composed of the actuator direction vectors is

$$\mathbf{Z} = \begin{bmatrix} 1 & 0 & 0 & 0 \\ 0 & 1 & 0 & 0 \end{bmatrix} \tag{34}$$

Then the coefficient matrix of the constraint and actuator forces, $\mathbf{A}^{\mathrm{T}}$ is

$$\mathbf{A}^{\mathrm{T}} = \begin{bmatrix} -r_1 s_1 - r_3 s_{13} & r_1 c_1 + r_3 c_{13} & 1 & 0 \\ r_2 s_2 + r_4 s_{24} & -r_2 c_2 - r_4 c_{24} & 0 & 1 \\ -r_3 s_{13} & r_3 c_{13} & 0 & 0 \\ r_4 s_{24} & -r_4 c_{24} & 0 & 0 \end{bmatrix} \tag{35}$$

The drive singularities are found from $|\mathbf{A}| = 0$ as $\sin(\theta_1 + \theta_3 - \theta_2 - \theta_4) = 0$, i.e. as the positions when points *A*, *B* and *D* become collinear. Hence, drive singularities occur inside the workspace and avoiding them limits the motion in the workspace. Defining a path for the operational point *P* which does not involve a singular position would restrict the motion to a portion of the workspace where point *D* remains on one side of the line joining *A* and *D*. In fact, in order to reach the rest of the workspace (corresponding to the other closure of the closed chain system) the manipulator has to pass through a singular position.

When the end point comes to $s = L_d = 0.80\,\mathrm{m}$, $\theta_1 + \theta_3$ becomes equal to $\pi + \theta_2 + \theta_4$, hence a drive singularity occurs. At this position the third row of $\mathbf{A}^{\mathrm{T}}$ becomes r_3 / r_4 times the fourth row. Then, for consistency of equation (8), the third row of the right hand side of equation (8) should also be r_3 / r_4 times the fourth row. The resulting consistency condition that the generalized accelerations must satisfy is obtained from equation (15) as

$$M_{31}\ddot{\theta}_1 - \frac{r_3}{r_4} M_{24}\ddot{\theta}_2 + M_{33}\ddot{\theta}_3 - \frac{r_3}{r_4} M_{44}\ddot{\theta}_4 = R_3 - \frac{r_3}{r_4} R_4 \tag{36}$$

Hence the time trajectory $s(t)$ of the deployment motion should be selected such that at the drive singularity the generalized accelerations satisfy equation (36).

An arbitrary trajectory that does not satisfy the consistency condition is not realizable. This is illustrated by considering an arbitrary third order polynomial for $s(t)$ having zero initial and final velocities, i.e. $s(t) = \frac{3Lt^2}{T^2} - \frac{2Lt^3}{T^3}$. The singularity position is reached when $t = 0.48\,\mathrm{s}$. The actuator torques are shown in Figure 2. The torques grow without bounds as the singularity is approached and become infinitely large at the singular position. (In Figure 2 the torques are out of range around the singular position.)

For the time function s(t), a polynomial is chosen which satisfies the consistency condition at the drive singularity in addition to having zero initial and final velocities. The time T_d when the singular position is reached and the velocity of the end point *P* at T_d, $v_P(T_d)$ can be arbitrarily chosen. The loop closure relations, the specified angle of the acceleration of *P* and the consistency condition constitute four independent equations for a unique solution of $\ddot{\theta}_i$, $i = 1,...,4$ at the singular position. Hence, using θ_i and $\dot{\theta}_i$ at T_d, the acceleration of *P* at T_d, $a_P(T_d)$ is uniquely determined. Consequently a sixth order polynomial is selected where $s(0) = 0$, $\dot{s}(0) = 0$, $s(T) = L$, $\dot{s}(T) = 0$, $s(T_d) = L_d$, $\dot{s}(T_d) = v_P(T_d)$ and $\ddot{s}(T_d) = a_P(T_d)$. T_d and $v_P(T_d)$ are chosen by trial and error to prevent any overshoot in s or $\dot{s}$. The values used are $T_d = 0.55\,\mathrm{s}$ and $v_P(T_d) = 3.0\,\mathrm{m/s}$, yielding $a_P(T_d) = 18.2\,\mathrm{m/s^2}$. $s(t)$ so obtained is given by equation (37) and shown in Figure 3.

$$s(t) = 30.496\,t^2 - 154.909\,t^3 + 311.148\,t^4 - 265.753\,t^5 + 81.318\,t^6 \tag{37}$$

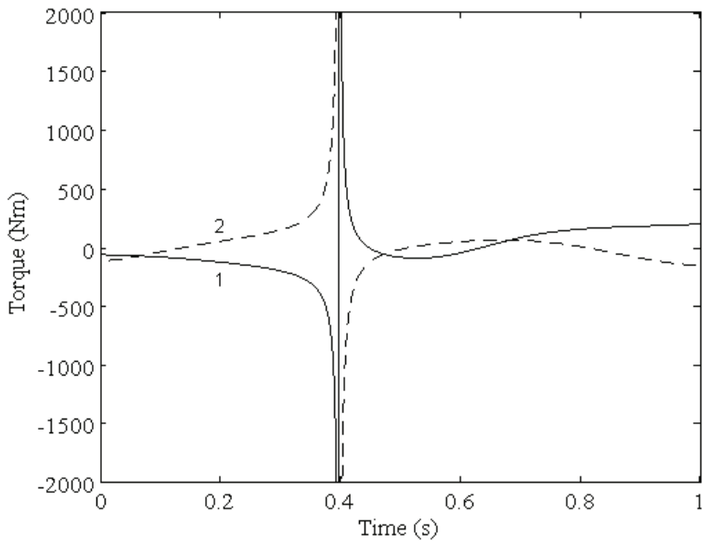

Figure 2. Motor torques for the trajectory not satisfying the consistency condition: 1. T_1 , 2. T_2

Furthermore, even when the consistency condition is satisfied, $\mathbf{A}^{\mathrm{T}}$ is ill-conditioned in the vicinity of the singular position, hence $\boldsymbol{\tau}$ cannot be found correctly from equation (8). Deletion of a linearly dependent equation in that neighborhood would cause task violations due to the removal of a task. For this reason the modified equation (17) is used to replace the dependent equation in the neighborhood of the singular position. The modified equation, which relates the actuator forces to the system jerks, takes the following form.

$$(\dot{A}_{31}^{\mathrm{T}} - \frac{r_3}{r_4}\dot{A}_{41}^{\mathrm{T}})\,\tau_1 + (\dot{A}_{32}^{\mathrm{T}} - \frac{r_3}{r_4}\dot{A}_{42}^{\mathrm{T}})\,\tau_2 = M_{31}\dddot{\theta}_1 - \frac{r_3}{r_4}M_{24}\dddot{\theta}_2 + M_{33}\dddot{\theta}_3 - \frac{r_3}{r_4}M_{44}\dddot{\theta}_4$$

$$+ \dot{M}_{31}\ddot{\theta}_1 - \frac{r_3}{r_4}\dot{M}_{24}\ddot{\theta}_2 + \dot{M}_{33}\ddot{\theta}_3 - \frac{r_3}{r_4}\dot{M}_{44}\ddot{\theta}_4 - \dot{R}_3 + \frac{r_3}{r_4}\dot{R}_4 \tag{38}$$

The coefficients of the constraint forces in eqn (38) are

$$\dot{A}_{31}^{\mathrm{T}} - \frac{r_3}{r_4}\dot{A}_{41}^{\mathrm{T}} = -r_3(\dot{\theta}_1 + \dot{\theta}_3)c_{13} - r_3(\dot{\theta}_2 + \dot{\theta}_4)c_{24} \tag{39a}$$

$$\dot{A}_{32}^{\mathrm{T}} - \frac{r_3}{r_4}\dot{A}_{42}^{\mathrm{T}} = -r_3(\dot{\theta}_1 + \dot{\theta}_3)s_{13} - r_3(\dot{\theta}_2 + \dot{\theta}_4)s_{24} \tag{39b}$$

which in general do not vanish at the singular position if the system is in motion.
Once the trajectory is chosen as above such that it renders the dynamic equations to be consistent at the singular position, the corresponding θ_i, $\dot{\theta}_i$ and $\ddot{\theta}_i$ are obtained from inverse kinematics, and when there is no actuation singularity, the actuator torques T_1 and

T_2 (along with the constraint forces λ_1 and λ_2) are obtained from equation (8). However in the neighborhood of the singular position, equation (22) is used in which the third row of equation (8) is replaced by the modified equation (38). The neighborhood of the singularity where equation (22) is utilized is taken as $\left|\theta_1+\theta_3-\theta_2-\theta_4-180^o\right|<\varepsilon=1^o$. The motor torques necessary to realize the task are shown in Figure 4. At the singular position the motor torques are found as $T_1=-138.07\,\text{Nm}$ and $T_2=-30.66\,\text{Nm}$. To test the validity of the modified equations, when the simulations are repeated with $\varepsilon=0.5^o$ and $\varepsilon=1.5^o$, no significant changes occur and the task violations remain less than 10^{-4} m.

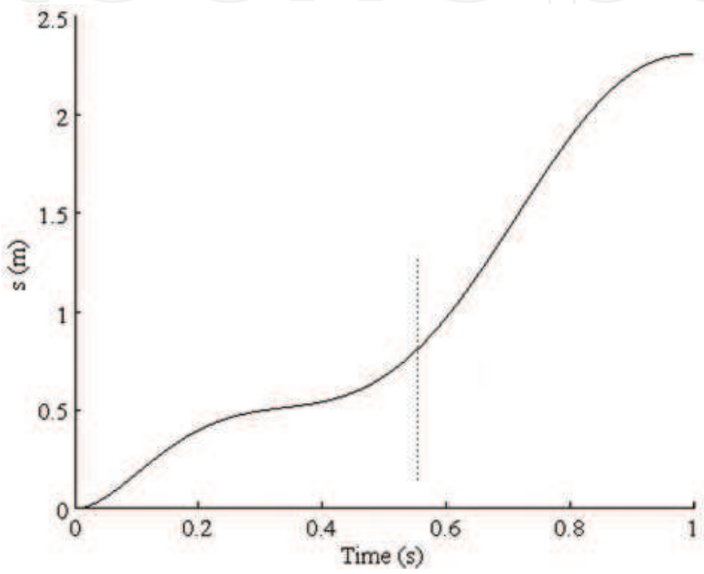

Figure 3. Time function satisfying the consistency condition.

4.2 Three degree of freedom 2-RPR planar parallel manipulator

The 2-*RPR* manipulator shown in Figure 5 has 3 degrees of freedom (*n*=3). Choosing the revolute joint at *D* for disconnection (among the passive joints) the joint variable vector of the open chain system is $\boldsymbol{\eta}=\begin{bmatrix}\theta_1 & \zeta_1 & \theta_2 & \zeta_2 & \theta_3\end{bmatrix}^{\mathrm{T}}$, where $\zeta_1=AB$ and $\zeta_2=CD$. The link dimensions of the manipulator are labelled as $a=AC$, $b=BD$, $c=BP$ and $\alpha=\angle PBD$. The position and orientation of the moving platform is $\mathbf{x}=\begin{bmatrix}x_P & y_P & \theta_3\end{bmatrix}^{\mathrm{T}}$ where x_P, y_P are the coordinates of the operational point of interest *P* in the moving platform.

The velocity level loop closure constraint equations are $\boldsymbol{\Gamma}^G\dot{\boldsymbol{\eta}}=\mathbf{0}$, where

$$\boldsymbol{\Gamma}^G=\begin{bmatrix}-\zeta_1\sin\theta_1 & \cos\theta_1 & \zeta_2\sin\theta_2 & -\cos\theta_2 & -b\sin\theta_3\\ \zeta_1\cos\theta_1 & \sin\theta_1 & -\zeta_2\cos\theta_2 & -\sin\theta_2 & b\cos\theta_3\end{bmatrix} \tag{40}$$

The prescribed position and orientation of the moving platform, $\mathbf{x}(t)$ represent the tasks of the manipulator. The task equations at velocity level are $\boldsymbol{\Gamma}^P\dot{\boldsymbol{\eta}}=\dot{\mathbf{x}}$ where

$$\mathbf{\Gamma}^{P} = \begin{bmatrix} -\zeta_1 \sin\theta_1 & \cos\theta_1 & 0 & 0 & -c\ \sin(\theta_3+\alpha) \\ \zeta_1 \cos\theta_1 & \sin\theta_1 & 0 & 0 & c\ \cos(\theta_3+\alpha) \\ 0 & 0 & 0 & 0 & 1 \end{bmatrix} \tag{41}$$

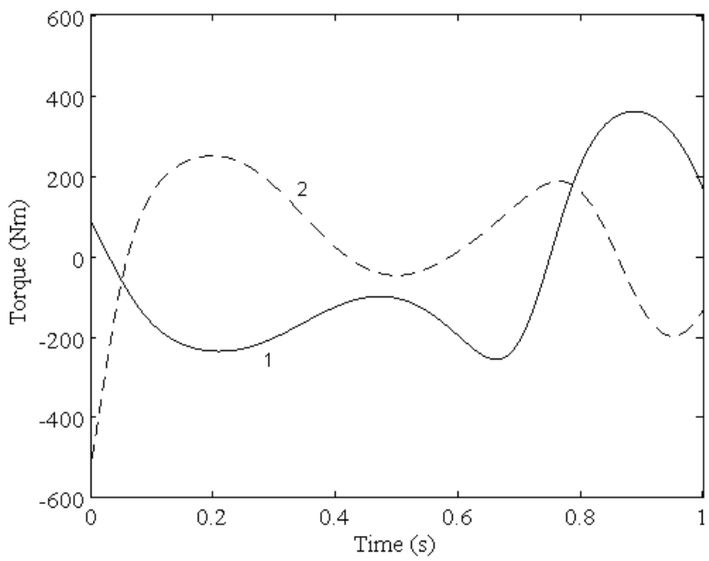

Figure 4. Motor torques for the trajectory satisfying the consistency condition: 1. T_1, 2. T_2.

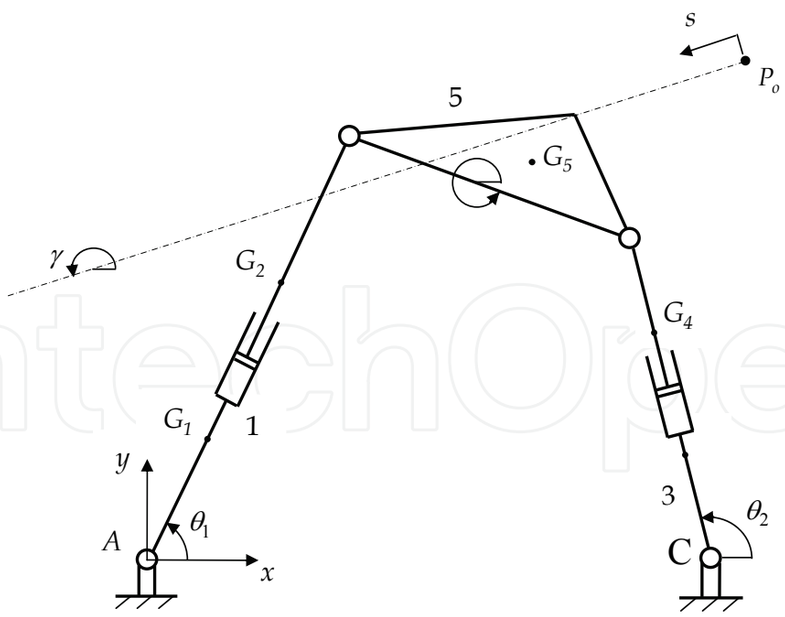

Figure 5. 2-*RPR* planar parallel manipulator.

Let the joints whose variables are θ_1, ζ_1 and ζ_2 be the actuated joints. The actuator force vector can be written as $\mathbf{T} = \begin{bmatrix} T_1 & F_1 & F_2 \end{bmatrix}^{\mathrm{T}}$ where T_1 is the motor torque corresponding to

θ_1, and F_1 and F_2 are the translational actuator forces corresponding to ζ_1 and ζ_2, respectively. Consider a deployment motion where the platform moves with a constant orientation given as $\theta_3 = 320^o$ and with point P having a trajectory $s(t)$ along a straight line whose angle with x-axis is $\gamma = 200^o$, starting from initial position $x_{P_o} = 0.800\,\mathrm{m}$, $y_{P_o} = 0.916\,\mathrm{m}$ (Figure 5). The time of the deployment motion is $T = 1\mathrm{s}$ and its length is $L = 1.5\,\mathrm{m}$. Hence the prescribed Cartesian motion of the platform can be written as

$$\mathbf{x} = \begin{bmatrix} x_P(t) \\ y_P(t) \\ \theta_3(t) \end{bmatrix} = \begin{bmatrix} x_{P_o} + s(t)\sin\gamma \\ y_{P_o} + s(t)\cos\gamma \\ 320^o \end{bmatrix} \tag{42}$$

The link dimensions and mass properties are arbitrarily chosen as follows. The link lengths are $AC = a = 1.0\mathrm{m}$, $BD = b = 0.4\mathrm{m}$, $BP = c = 0.2\,\mathrm{m}$, $\angle PBD = \alpha = 0$. The masses and the centroidal moments of inertia are $m_1 = 2\,\mathrm{kg}$, $m_2 = 1.5\,\mathrm{kg}$, $m_3 = 2\,\mathrm{kg}$, $m_4 = 1.5\,\mathrm{kg}$, $m_5 = 1.0\,\mathrm{kg}$, $I_1 = 0.05\,\mathrm{kg\,m^2}$, $I_2 = 0.03\,\mathrm{kg\,m^2}$, $I_3 = 0.05\,\mathrm{kg\,m^2}$, $I_4 = 0.03\,\mathrm{kg\,m^2}$ and $I_5 = 0.02\,\mathrm{kg\,m^2}$. The mass center locations are given by $AG_1 = g_1 = 0.15\,\mathrm{m}$, $BG_2 = g_2 = 0.15\,\mathrm{m}$, $CG_3 = g_3 = 0.15\,\mathrm{m}$, $DG_4 = g_4 = 0.15\,\mathrm{m}$, $BG_5 = g_5 = 0.2\,\mathrm{m}$ and $\angle G_5BD = \beta = 0$.

The generalized mass matrix **M** and the generalized inertia forces involving the second order velocity terms **R** are

$$\mathbf{M} = \begin{bmatrix} M_{11} & 0 & 0 & 0 & M_{15} \\ 0 & M_{22} & 0 & 0 & M_{25} \\ 0 & 0 & M_{33} & 0 & 0 \\ 0 & 0 & 0 & M_{44} & 0 \\ M_{51} & M_{52} & 0 & 0 & M_{55} \end{bmatrix}, \quad \mathbf{R} = \begin{bmatrix} R_1 \\ R_2 \\ R_3 \\ R_4 \\ R_5 \end{bmatrix} \tag{43}$$

where M_{ij} and R_i are given in the Appendix.

For the set of actuators considered, the actuator direction matrix **Z** is

$$\mathbf{Z} = \begin{bmatrix} 1 & 0 & 0 & 0 & 0 \\ 0 & 1 & 0 & 0 & 0 \\ 0 & 0 & 0 & 1 & 0 \end{bmatrix} \tag{44}$$

Hence, $\mathbf{A}^{\mathrm{T}}$ becomes

$$\mathbf{A}^{\mathrm{T}} = \begin{bmatrix} -\zeta_1\sin\theta_1 & \zeta_1\cos\theta_1 & 1 & 0 & 0 \\ \cos\theta_1 & \sin\theta_1 & 0 & 1 & 0 \\ \zeta_2\sin\theta_2 & -\zeta_2\cos\theta_2 & 0 & 0 & 0 \\ -\cos\theta_2 & -\sin\theta_2 & 0 & 0 & 1 \\ -b\sin\theta_3 & b\cos\theta_3 & 0 & 0 & 0 \end{bmatrix} \tag{45}$$

Since $|\mathbf{A}| = b\,\zeta_2 \sin(\theta_2 - \theta_3)$, drive singularities occur when $\zeta_2 = 0$ or $\sin(\theta_2 - \theta_3) = 0$. Noting that ζ_2 does not become zero in practice, the singular positions are those positions where points *B*, *D* and *C* become collinear.

Hence, drive singularities occur inside the workspace and avoiding them limits the motion in the workspace. Avoiding singular positions where $\theta_2 - \theta_3 = \pm n\pi \quad (n = 0,1,2,...)$ would restrict the motion to a portion of the workspace where point *D* is always on the same side of the line *BC*. This means that in order to reach the rest of the workspace (corresponding to the other closure of the closed chain system) the manipulator has to pass through a singular position.

When point *P* comes to $s = L_d = 0.662\,\text{m}$, a drive singularity occurs since θ_2 becomes equal to $\theta_3 + \pi$. At this position the third and fifth rows of $\mathbf{A}^{\mathrm{T}}$ become linearly dependent as $A_{3j}^T - \frac{\zeta_2}{b} A_{5j}^T = 0$, $j = 1,...,5$. The consistency condition is obtained as below

$$M_{33}\ddot{\theta}_2 - \frac{\zeta_2}{b}(M_{51}\ddot{\theta}_1 + M_{52}\ddot{\zeta}_1 + M_{55}\ddot{\theta}_3) = R_3 - \frac{\zeta_2}{b} R_5 \tag{46}$$

The desired trajectory should be chosen in such a way that at the singular position the generalized accelerations should satisfy the consistency condition.

If an arbitrary trajectory that does not satisfy the consistency condition is specified, then such a trajectory is not realizable. The actuator forces grow without bounds as the singular position is approached and become infinitely large at the singular position. This is illustrated by using an arbitrary third order polynomial for $s(t)$ having zero initial and final velocities, i.e. $s(t) = \frac{3Lt^2}{T^2} - \frac{2Lt^3}{T^3}$. The singularity occurs when $t = 0.46\,\text{s}$. The actuator forces are shown in Figures 6 and 7. (In the figures the forces are out of range around the singular position.)

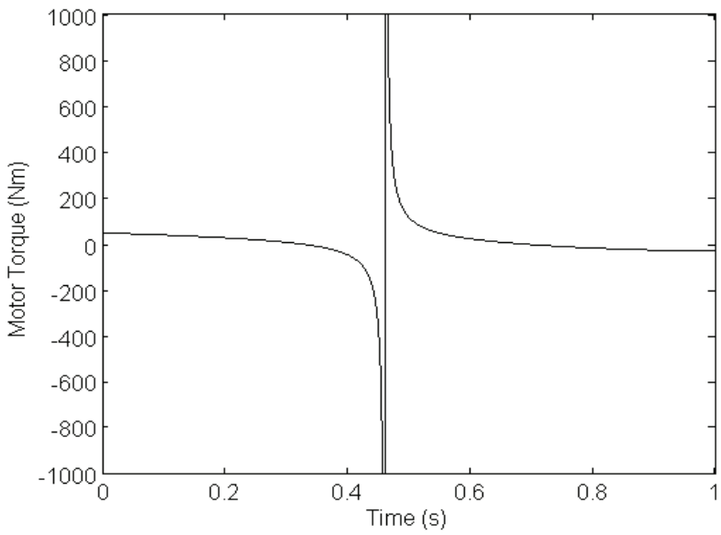

Figure 6. Motor torque for the trajectory not satisfying the consistency condition.

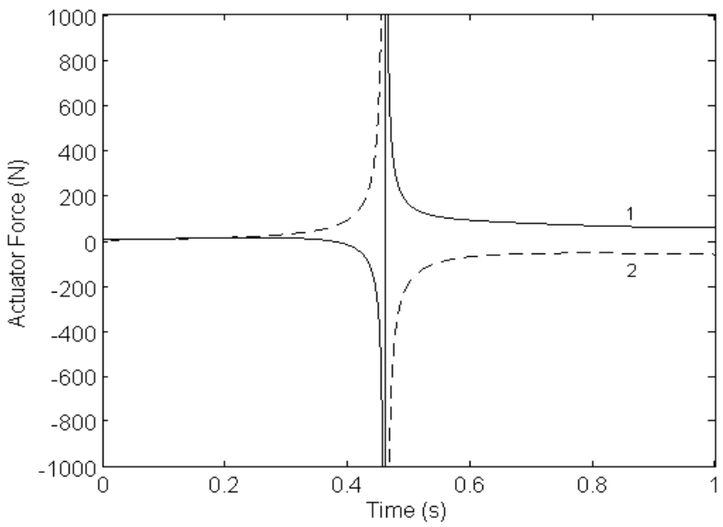

Figure 7. Actuator forces for the trajectory not satisfying the consistency cond.: 1. F_1 , 2. F_2 .

For the time function $s(t)$ a polynomial is chosen that renders the dynamic equations to be consistent at the singular position in addition to having zero initial and final velocities. The time T_d when singularity occurs and the velocity of the end point when $t = T_d$, $v_P(T_d)$ can be arbitrarily chosen. The acceleration level loop closure relations, the specified angle of the acceleration of P ($\gamma = 200^o$), the specified angular acceleration of the platform $(\ddot{\theta}_3 = 0)$ and the consistency condition constitute five independent equations for a unique solution of $\ddot{\eta}_i$, $i = 1,...,5$ at the singular position. Hence, using $\boldsymbol{\eta}$ and $\dot{\boldsymbol{\eta}}$ at T_d , the acceleration of P at T_d , $a_P(T_d)$ is uniquely determined. Consequently a sixth order polynomial is selected where $s(0) = 0$, $\dot{s}(0) = 0$, $s(T) = L$, $\dot{s}(T) = 0$, $s(T_d) = L_d$, $\dot{s}(T_d) = v_P(T_d)$ and $\ddot{s}(T_d) = a_P(T_d)$. The values used for T_d and $v_P(T_d)$ are $0.62\,\mathrm{s}$ and $1.7\,\mathrm{m/s}$ respectively, yielding $a_P(T_d) = 10.6\,\mathrm{m/s^2}$. $s(t)$ so obtained is shown in Figure 8 and given by equation (47).

$$s(t) = 20.733\,t^2 - 87.818\,t^3 + 146.596\,t^4 - 103.669\,t^5 + 25.658\,t^6 \tag{47}$$

Bad choices for T_d and $v_P(T_d)$ would cause local peaks in $s(t)$ implying back and forth motion of point P during deployment along its straight line path.
However, even when the equations are consistent, in the neighborhood of the singular positions $\mathbf{A}^{\mathrm{T}}$ is ill-conditioned, hence $\boldsymbol{\tau}$ cannot be found correctly from equation (8). This problem is eliminated by utilizing the modified equation valid in the neighborhood of the singular position. The modified equation (17) takes the following form

$$B_j\,\tau_j = Q \qquad\qquad j = 1,2 \tag{48}$$

where

$$B_1 = \dot{A}_{31}^T - \frac{\zeta_2}{b}\dot{A}_{51}^T - \frac{\dot{\zeta}_2}{b}A_{51}^T\,, \qquad B_2 = \dot{A}_{32}^T - \frac{\zeta_2}{b}\dot{A}_{52}^T - \frac{\dot{\zeta}_2}{b}A_{52}^T \tag{49a}$$

$$Q = M_{33}\dddot{\theta}_2 - \frac{\zeta_2}{b}(M_{51}\dddot{\theta}_1 + M_{52}\dddot{\zeta}_1 + M_{55}\dddot{\theta}_3) + \dot{M}_{33}\ddot{\theta}_2 - \frac{\zeta_2}{b}(\dot{M}_{51}\ddot{\theta}_1 + \dot{M}_{52}\ddot{\zeta}_1$$

$$+\dot{M}_{55}\ddot{\theta}_3) - \frac{\dot{\zeta}_2}{b}(M_{51}\ddot{\theta}_1 + M_{52}\ddot{\zeta}_1 + M_{55}\ddot{\theta}_3) \; -\dot{R}_3 + \frac{\zeta_2}{b}\dot{R}_5 + \frac{\dot{\zeta}_2}{b}R_5 \tag{49b}$$

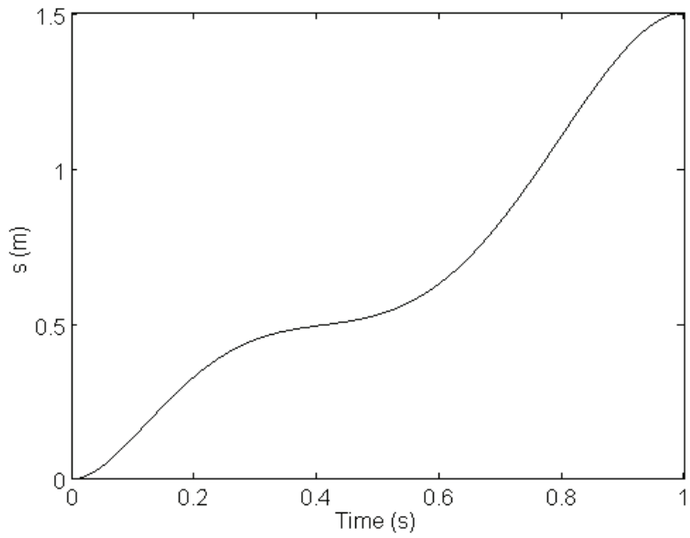

Figure 8. A time function that satisfies the consistency condition.

Once the trajectory is specified, the corresponding $\boldsymbol{\eta}$, $\dot{\boldsymbol{\eta}}$ and $\ddot{\boldsymbol{\eta}}$ are obtained from inverse kinematics, and when there is no actuation singularity, the actuator forces T_1, F_1 and F_2 (and the constraint forces λ_1 and λ_2) are obtained from equation (8). However in the neighborhood of the singularity, **A** is ill-conditioned. So the unknown forces are obtained from equation (22) which is obtained by replacing the third row of equation (8) by the modified equation (48). The neighborhood of the singular position where equation (22) is utilized is taken as $\left|\theta_2 - \theta_3 + 180^o\right| < \varepsilon = 0.5^o$. The motor torques and the translational actuator forces necessary to realize the task are shown in Figures 9 and 10, respectively. At the singular position the actuator forces are $T_1 = 30.31$ Nm, $F_1 = 26.3$ N and $F_2 = 1.61$ N. The joint displacements under the effects of the actuator forces are given in Figures 11 and 12. To test the validity of the modified equations in a larger neighborhood, when the simulations are repeated with $\varepsilon = 1^o$, no significant changes are observed, the task violations remaining less than 10^{-5} m.

5. Conclusions

A general method for the inverse dynamic solution of parallel manipulators in the presence of drive singularities is developed. It is shown that at the drive singularities, the actuator forces cannot influence the end-effector accelerations instantaneously in certain directions. Hence the end-effector trajectory should be chosen to satisfy the consistency of the dynamic

equations when the coefficient matrix of the drive and constraint forces, **A** becomes singular. The satisfaction of the consistency conditions makes the trajectory to be realizable by the actuators of the manipulator, hence avoids the divergence of the actuator forces.

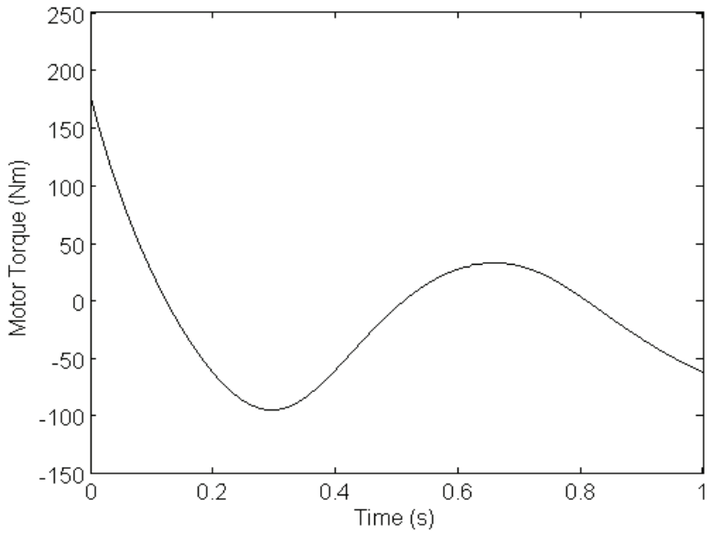

Figure 9. Motor torque for the trajectory satisfying the consistency condition

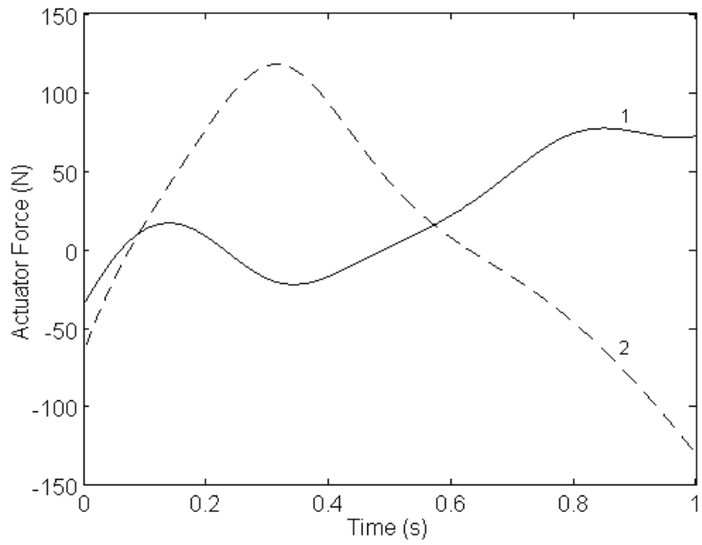

Figure 10. Actuator forces for the trajectory satisfying the consistency condition: 1. F_1 , 2. F_2

To avoid the problems related to the ill-condition of the force coefficient matrix, **A** in the neighborhood of the drive singularities, a modification of the dynamic equations is made using higher order derivative information. Deletion of the linearly dependent equation in that neighborhood would cause task violations due to the removal of a task. For this reason the modified equation is used to replace the dependent equation yielding a full rank force coefficient matrix.

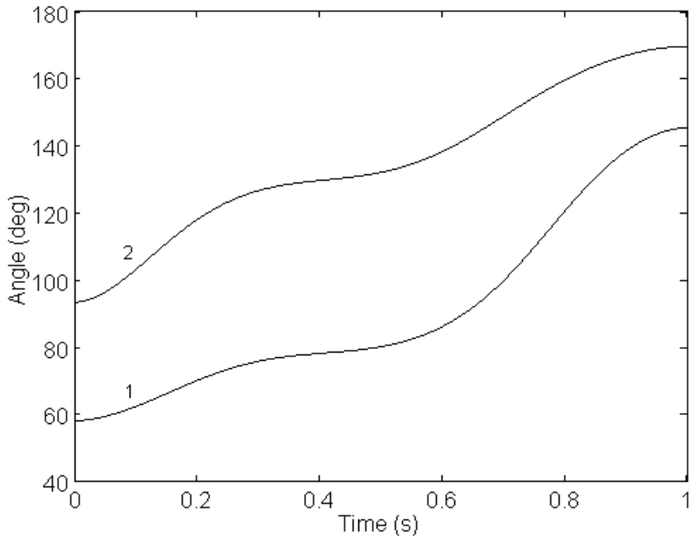

Figure 11. Rotational joint displacements: 1. θ_1 , 2. θ_2 .

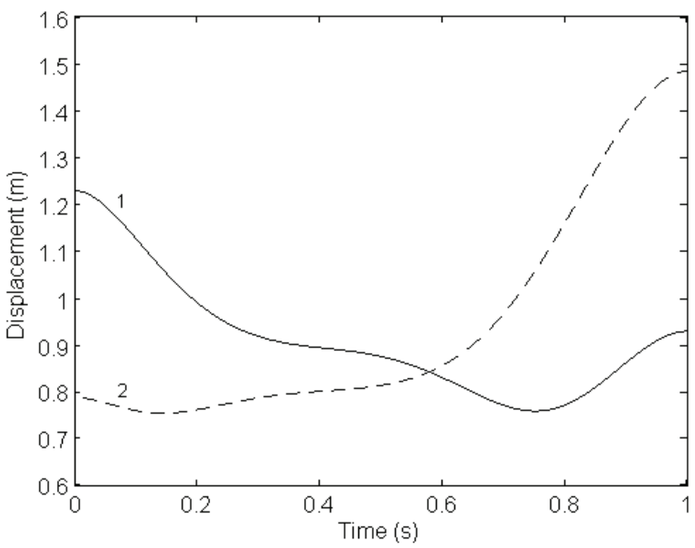

Figure 12. Translational joint displacements: 1. ζ_1 , 2. ζ_2 .

6. References

Alıcı, G. (2000). Determination of singularity contours for five-bar planar parallel manipulators, *Robotica,* Vol. 18, No. 5, (September 2000) 569-575.

Daniali, H.R.M.; Zsombor-Murray, P.J. & Angeles, J. (1995). Singularity analysis of planar parallel manipulators, *Mechanism and Machine Theory,* Vol. 30, No. 5, (July 1995) 665-678.

Di Gregorio, R. (2001). Analytic formulation of the 6-3 fully-parallel manipulator's singularity determination, *Robotica,* Vol. 19, No. 6, (September 2001) 663-667.

Gao, F.; Li, W.; Zhao, X.; Jin, Z. & Zhao, H. (2002). New kinematic structures for 2-, 3-, 4-, and 5-DOF parallel manipulator designs, *Mechanism and Machine Theory,* Vol. 37**,** No. 11, (November 2002) 1395-1411.

Gunawardana, R. & Ghorbel, F. (1997). PD control of closed-chain mechanical systems: an experimental study, *Proceedings of the Fifth IFAC Symposium on Robot Control*, Vol. 1, 79-84, Nantes, France, September 1997, Cambridge University Press, New York.

Ider, S.K. (2004). Singularity robust inverse dynamics of planar 2-RPR parallel manipulators, *Proceedings of the Institution of Mechanical Engineers, Part C: Journal of Mechanical Engineering Science,* Vol. 218, No. 7, (July 2004) 721-730.

Ider, S.K. (2005). Inverse dynamics of parallel manipulators in the presence of drive singularities, *Mechanism and Machine Theory,* Vol. 40, No. 1, (January 2005) 33-44.

Ji, Z. (2003) Study of planar three-degree-of-freedom 2-RRR parallel manipulators, *Mechanism and Machine Theory,* Vol. 38, No. 5, (May 2003) 409-416.

Kong, X. & Gosselin, C.M. (2001). Forward displacement analysis of third-class analytic 3-RPR planar parallel manipulators, *Mechanism and Machine Theory,* Vol. 36, No. 9, (September 2001) 1009-1018.

Merlet, J.-P. (1999). Parallel Robotics: Open Problems, *Proceedings of Ninth International Symposium of Robotics Research*, 27-32, Snowbird, Utah, October 1999, Springer-Verlag, London.

Sefrioui, J. & Gosselin, C.M. (1995). On the quadratic nature of the singularity curves of planar three-degree-of-freedom parallel manipulators, *Mechanism and Machine Theory,* Vol. 30, No. 4, (May 1995) 533-551.

Appendix

The elements of **M** and ***R*** of the 2-RPR parallel manipulator shown in equation (41) are given below, where m_i, $i=1,...,5$ are the masses of the links, I_i, $i=1,...,5$ are the centroidal moments of inertia of the links and the locations of the mass centers G_i, $i=1,...,5$ are indicated by $g_1 = AG_1$, $g_2 = BG_2$, $g_3 = CG_3$, $g_4 = DG_4$, $g_5 = BG_5$ and $\beta = \angle G_5BD$.

$$M_{11} = m_1 g_1^2 + I_1 + m_2(\zeta_1 - g_2)^2 + I_2 + m_5\zeta_1^2 \tag{A1}$$

$$M_{15} = m_5\zeta_1 g_5 \cos(\theta_1 - \theta_3 - \beta) \tag{A2}$$

$$M_{22} = m_2 + m_3 \tag{A3}$$

$$M_{25} = m_5 g_5 \sin(\theta_1 - \theta_3 - \beta) \tag{A4}$$

$$M_{33} = m_3 g_3^2 + I_3 + m_4(\zeta_2 - g_4)^2 + I_4 \tag{A5}$$

$$M_{44} = m_4 \tag{A6}$$

$$M_{51} = m_5\zeta_1 g_5 \cos(\theta_1 - \theta_3 - \beta) \tag{A7}$$

$$M_{52} = m_5 g_5 \sin(\theta_1 - \theta_3 - \beta) \tag{A8}$$

$$M_{55} = m_5 g_5^2 + I_5 \tag{A9}$$

$$R_1 = 2m_2(\zeta_1 - g_2)\dot{\zeta}_1\dot{\theta}_1 + m_5\zeta_1 g_5\dot{\theta}_3^2 \sin(\theta_1 - \theta_3 - \beta) + [m_1 g_1 + m_2(\zeta_1 - g_2) + m_5\zeta_1]g\cos\theta_1 \tag{A10}$$

$$R_2 = -m_5 g_5\dot{\theta}_3^2 \cos(\theta_1 - \theta_3 - \beta) - m_2(\zeta_1 - g_2)\dot{\theta}_1^2 - m_5\zeta_1\dot{\theta}_1^2 + (m_2 + m_5)g\sin\theta_1 \tag{A11}$$

$$R_3 = 2m_4(\zeta_2 - g_4)\dot{\zeta}_2\dot{\theta}_2 + [m_3 g_3 + m_4(\zeta_2 - g_4)]g\cos\theta_2 \tag{A12}$$

$$R_4 = -m_4(\zeta_2 - g_4)\dot{\theta}_2^2 + m_4 g\sin\theta_2 \tag{A13}$$

$$R_5 = m_5 g_5[2\dot{\zeta}_1\dot{\theta}_1 \cos(\theta_1 - \theta_3 - \beta) - \zeta_1\dot{\theta}_1^2 \sin(\theta_1 - \theta_3 - \beta) + g\cos(\theta_3 + \beta)] \tag{A14}$$

Parallel Manipulators, New Developments

Edited by Jee-Hwan Ryu

ISBN 978-3-902613-20-2

Hard cover, 498 pages

Publisher I-Tech Education and Publishing

Published online 01, April, 2008

Published in print edition April, 2008

Parallel manipulators are characterized as having closed-loop kinematic chains. Compared to serial manipulators, which have open-ended structure, parallel manipulators have many advantages in terms of accuracy, rigidity and ability to manipulate heavy loads. Therefore, they have been getting many attentions in astronomy to flight simulators and especially in machine-tool industries.The aim of this book is to provide an overview of the state-of-art, to present new ideas, original results and practical experiences in parallel manipulators. This book mainly introduces advanced kinematic and dynamic analysis methods and cutting edge control technologies for parallel manipulators. Even though this book only contains several samples of research activities on parallel manipulators, I believe this book can give an idea to the reader about what has been done in the field recently, and what kind of open problems are in this area.

InTech Europe

University Campus STeP Ri
Slavka Krautzeka 83/A
51000 Rijeka, Croatia
Phone: +385 (51) 770 447
Fax: +385 (51) 686 166
www.intechopen.com

InTech China

Unit 405, Office Block, Hotel Equatorial Shanghai
No.65, Yan An Road (West), Shanghai, 200040, China
中国上海市延安西路65号上海国际贵都大饭店办公楼405单元
Phone: +86-21-62489820
Fax: +86-21-62489821

IntechOpen